Protein Kinase A Catalytic Subunit Alters Cardiac Mitochondrial Redox State and Membrane Potential Via the Formation of Reactive Oxygen Species

Shiro Nagasaka, MD; Hideki Katoh, MD; Chun Feng Niu, MD;
Saori Matsui, MD; Tsuyoshi Urushida, MD; Hiroshi Satoh, MD;
Yasuhide Watanabe, PhD*; Hideharu Hayashi, MD

Background The identification of protein kinase A (PKA) anchoring proteins on mitochondria implies a direct effect of PKA on mitochondrial function. However, little is known about the relationship between PKA and mitochondrial metabolism.

Methods and Results The effects of PKA on the mitochondrial redox state (flavin adenine dinucleotide (FAD)), mitochondrial membrane potential (Δ_m) and reactive oxygen species (ROS) production were investigated in saponin-permeabilized rat cardiomyocytes. The PKA catalytic subunit (PKA$_{cat}$; 50 unit/ml) increased FAD intensities by $56.6\pm7.9\%$ (p<0.01), 2'7'-dichlorofluorescin diacetate (DCF) intensities by 10.5 ± 3.3 fold (p<0.01) and depolarized Δ_m to $48.1\pm9.5\%$ of the control (p<0.01). Trolox (a ROS scavenger; 100μmol/L) inhibited PKA$_{cat}$-induced Δ_m, FAD and DCF alteration. PKA$_{cat}$-induced Δ_m depolarization was inhibited by an inhibitor of the inner membrane anion channel (IMAC), 4,4'-diisothiocyanatostilbene-2,2'-disulfonic acid (DIDS: 1μmol/L) but not by an inhibitor of mitochondrial permeability transition pore (mPTP), cyclosporine A (100 nmol/L).

Conclusions PKA$_{cat}$ alters FAD and Δ_m via mitochodrial ROS generation, and PKA$_{cat}$-induced Δ_m depolarization was not caused by mPTP but rather by DIDS-sensitive mechanisms, which could be caused by opening of the IMAC. The effects of PKA on mitochondrial function could be related to myocardial function under the condition of extensive -adrenergic stimulation. (*Circ J* 2007; **71**: 429–436)

Key Words: Inner membrane anion channel; Mitochondrial membrane potential; Mitochondrial respiratory chain; Protein kinase A; Reactive oxygen species

Beta-adrenergic receptors (BAR) play a central role in sympathetic regulation of cardiac function and mediate the normal physiological responses of increased heart rate and contractility in response to exercise and stress. Stimulation of BAR induces chronotropic, inotropic and relaxant effects via the Gs-adenylate cyclase-cAMP-protein kinase A (PKA) pathway. The PKA catalytic subunit (PKA$_{cat}$), an activated form of PKA, phosphorylates functional proteins such as Ca^{2+} channels, sarcoplasmic reticulum Ca^{2+}-ATPase and ryanodine receptors.[1–3]

In heart failure, sympathetic activity increases to compensate for the impaired cardiac contractility; however, chronic and sustained activation of BAR under pathological conditions is regarded to be maladaptive.[4] Beta-adrenergic blockade prevents or reverses the structural and functional changes that develop during the progression of heart failure and has become the standard therapy for heart failure.[5]

The adverse effect of excessive BAR agonists, such as isoproterenol (ISO), and other catecholamines on myocytes is associated with abnormal Ca^{2+} regulation and excessive energy demand caused by a large increase in cardiac work.[6] On the other hand, subcutaneous administration of ISO reportedly depolarized the cardiac mitochondrial membrane potential (Δ_m) and decreased the respiratory state 3 activity, suggesting ISO-induced mitochondrial dysfunction.[7]

It has been reported that BAR activation provokes oxidative stress in the heart[8] and the cell damage by catecholamines has been attributed to their oxidation metabolites, which antioxidation prevents.[9] Furthermore, a BAR blocking agent, carvedilol, has been reported to inhibit mitochondrial superoxide production.[10] However, the sources and precise mechanisms of reactive oxygen species (ROS) generation by catecholamines are still in debate.

Recently, PKA anchoring proteins (AKAP) and phosphorylation sites for the substrates of PKA were identified on the mitochondrial outer membrane.[11,12] AKAP plays an important role as the delivery system of cAMP or PKA to the localized domains of targeting proteins. Although PKA can phosphorylate many substrates in vitro, PKA in vivo may preferentially target the sites that are near AKAPs, which implies that there could be a direct effect of PKA on mitochondrial function by phosphorylating as yet unknown proteins on the mitochondrial membrane. In isolated mitochondria, PKA activates proteins of the respiratory chain complex I;[13] however, relatively little is known about the relationship between Δ_m, the redox state and PKA in the cell level.

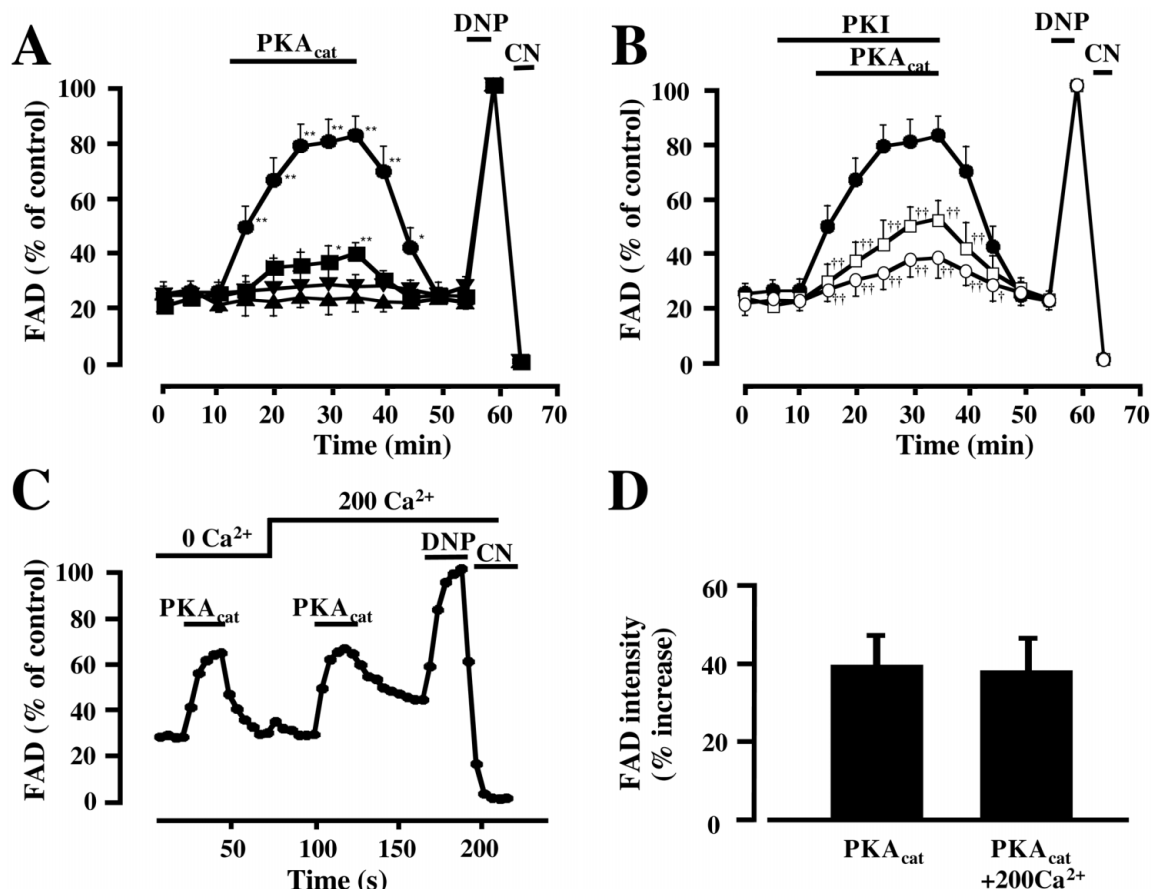The aims of this study were to (1) determine the effect of PKA on mitochondrial function, (2) clarify whether PKA

Fig 1. Effects of PKAcat on the mitochondrial redox state (FAD) in permeabilized myocytes. (A) Time course of the changes in the FAD signal (, no PKAcat; n=6, 2 rats; , 5 units/ml; n=5, 1 rat; , 25 units/ml; n=8, 2 rats; , 50 units/ml; n=13, 4 rats). (B) Changes in the FAD signal during perfusion of PKAcat in the absence (, n=13, 4 rats) or presence of PKI (□, 20 μmol/L; n=10, 2 rats; ○, 80 μmol/L; n=5, 1 rat). (C) Representative recording of the changes in FAD fluorescence with 50 units/ml PKAcat in the absence or presence of 200 nmol/L Ca^{2+}. (D) FAD fluorescence after 20 min perfusion of PKAcat in the absence (PKAcat; n=6, 2 rats) or presence (PKAcat+200 Ca^{2+}; n=6, 2 rats) of 200 nmol/L Ca^{2+}. Each signal was calibrated as 100% for DNP (100 μmol/L)-induced maximum oxidation and as 0% for sodium cyanide (CN: 2 mmol/L)-induced complete reduction. Values are mean±SEM. *p<0.05 vs no PKAcat by ANOVA. **p<0.01 vs no PKAcat by ANOVA. †p<0.05 vs 50 units/ml PKAcat by ANOVA. ††p<0.01 vs 50 units/ml PKAcat by ANOVA. DNP, 2,4-dinitrophenol; FAD, flavin adenine dinucleotide; PKAcat, catalytic subunit of protein kinase A; PKI, PKA inhibitor fragment 14–24 trifluoroacetate salt.

induces ROS generation in mitochondria and (3) examine how the generated ROS contribute to the changes in mitochondrial function.

Methods

Cells Isolation and Permeabilization of the Cell

This investigation conforms with the Guide for the Care and Use of Laboratory Animals published by the US National Institutes of Health (NIH Publication No. 85-23, revised 1996). Isolated myocytes from male Sprague-Dawley rats (250–300 g) were obtained by enzymatic dissociation and the cells were kept in modified Kraft-Brühe solution,[14–16] which contained (mmol/L) 70 KOH, 40 KCl, 20 KH_2PO_4, 3 $MgCl_2$, 50 glutamic acid, 10 glucose, 10 HEPES, and 0.5 EGTA (pH 7.4 with KOH). Just before the experiments, the cells were placed in a chamber and perfused with normal Tyrode solution, composed of (mmol/L) 143 NaCl, 5.4 KCl, 0.5 $MgCl_2$, 0.25 NaH_2PO_4, 1 $CaCl_2$, 5.6 glucose and 5 HEPES (pH 7.4 with NaOH). All experiments were conducted at room temperature (22°C)

within 6 h of cell isolation. For the permeabilization of the sarcolemmal membrane, the cells were perfused with saponin (0.05 mg/ml) in a Ca^{2+}-free internal solution, which contained (mmol/L) 50 KCl, 80 K-asparate, 2 Na-pyruvate, 20 HEPES, 3 $MgCl_2$–$6H_2O$, 2 Na_2ATP, 3 EGTA (pH 7.3 with KOH). After the sarcolemmal membrane was permeabilized, the concentration of free Ca^{2+} in the internal solution ([Ca^{2+}]c) was increased according to the experimental protocol. [Ca^{2+}]c was obtained by mixing EGTA and $CaCl_2$, calculated with a computer program (WIN MAXC, provided by Stanford University). Experiments were performed using a laser scanning confocal microscope (LSM 510, Zeiss) coupled to an inverted microscope (Axiovert S100, Zeiss) with a ×63 water-immersion objective lens ([NA]=1.3; Zeiss).

Imaging of Flavin Adenine Dinucleotide (FAD) Oxidation

The mitochondrial redox state of a single myocyte was assessed by measuring FAD-linked protein fluorescence. Endogenous FAD autofluorescence was excited at 488 nm with an argon ion laser and fluorescence was collected
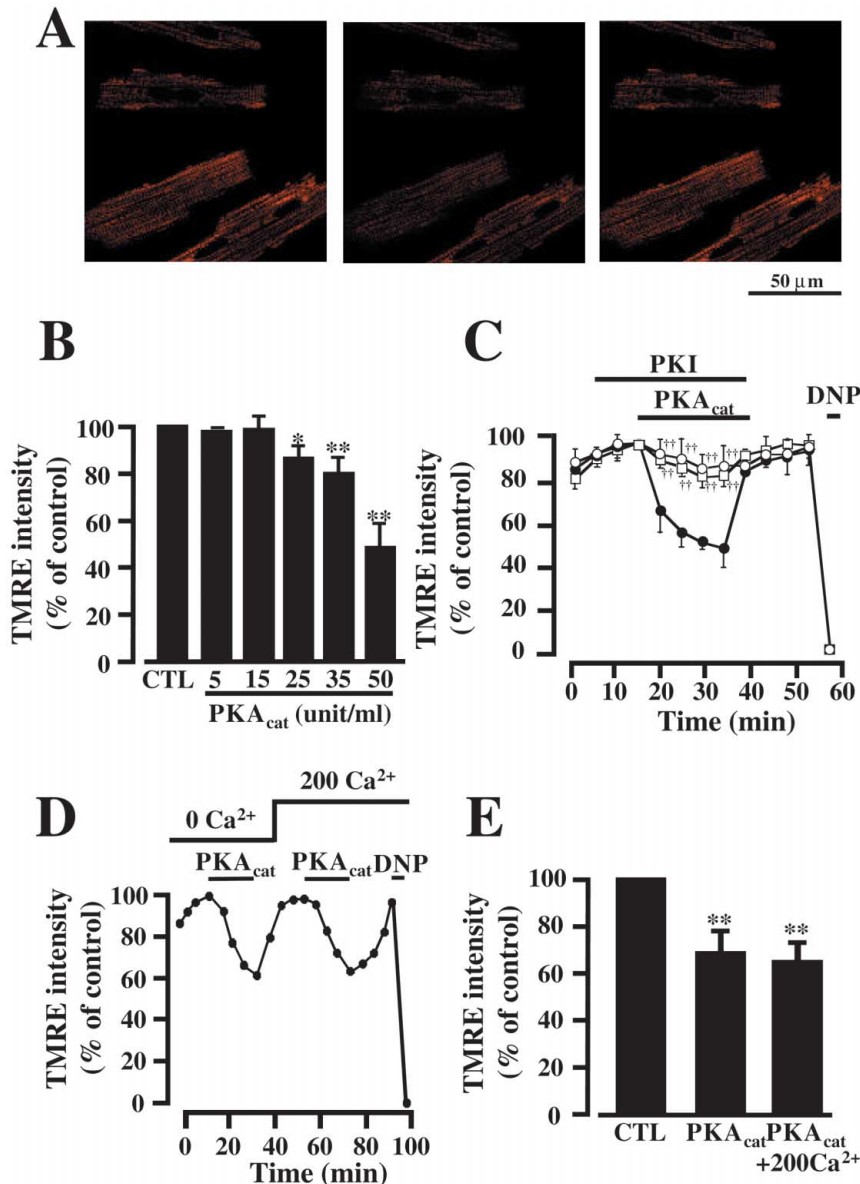
Fig 2. Effects of PKA$_{cat}$ on the mitochondrial membrane potential ($\Delta\Psi_m$) in permeabilized myocytes (A) 2-D images of tetramethylrhodamine ethyl ester (TMRE) were obtained before (Left), after administration (Center) and after the washout of PKA$_{cat}$ (Right). (B) Dose-dependent effects of PKA$_{cat}$ on TMRE fluorescence after 20 min perfusion of PKA$_{cat}$ (n=4–6, 1–2 rats). (C) Time course of the changes in the TMRE signal during perfusion of PKA$_{cat}$ in the absence ($\bullet$, n=6, 2 rats) or presence of PKI ($\square$, 20μmol/L; n=7, 2 rats; $\bigcirc$, 80μmol/L; n=6, 1 rats). (D) Representative recording of the changes in TMRE fluorescence with PKA$_{cat}$ in the absence or presence of 200 nmol/L Ca^{2+}. (E) Changes in TMRE fluorescence before (CTL) and 20 min after the perfusion of PKA$_{cat}$ in the absence (PKA$_{cat}$; n=5, 1 rat) or presence (PKA$_{cat}$+200 Ca^{2+}; n=5, 1 rat) of 200 nmol/L Ca^{2+}. Each signal was calibrated as 100% for intensities just before the application of PKA$_{cat}$. Values are mean ± SEM. *p<0.05 vs CTL by paired t-test, **p<0.01 vs CTL by paired t-test, ††p<0.01 vs 50 units/ml PKA$_{cat}$ by ANOVA. See Fig 1 for other abbreviations.

through a 505-nm long-pass filter. Two-dimensional (D) images were acquired at 1–5 min intervals. The FAD signal decreased to a minimum in the presence of a cytochrome oxidase inhibitor cyanide (CN$^-$, 2 mmol/L), and increased when exposed to a mitochondrial uncoupler 2,4-dinitrophenol (DNP, 100μmol/L). CN$^-$ and DNP are expected to cause maximum reduction and oxidation, respectively![6] Each signal was calibrated as 0% for CN$^-$-induced complete reduction and as 100% for DNP. Fluorescence intensity was integrated over the regions of interest (ROI: 30×30 pixels), excluding the nuclei and the edge of the cell.

Measurement of $\Delta\Psi_m$

For the measurement of $\Delta\Psi_m$, permeabilized myocytes were loaded with a continuous perfusion of fluorescent indicator tetramethylrhodamine ethyl ester (TMRE: 20 nmol/L). TMRE was excited at 543 nm with a helium–neon laser, and the emission signals were collected through a 560-nm long-pass filter. Data were presented as the % of the TMRE signal before the administration of drugs. Fluorescence intensity was integrated over the ROI (30×30 pixels), exclud-

ing the nuclei and the edge of the cell.

Measurement of ROS in Skinned Myocytes

For the measurement of the generation of ROS, permeabilized myocytes were loaded with a continuous perfusion of a fluorescent indicator 2'7'-dichlorofluorescin diacetate (DCF: 10μmol/L). Cells were excited with the 514 nm line of the argon laser, and the emission signals were collected through a 530-nm long-pass filter. The fluorescent intensities at the identical ROI (30×30 pixels) were monitored every 1–5 min to analyze the changes in the DCF signals.

Chemicals and Data Analyses

All chemicals were obtained from Sigma (St Louis, MO, USA) and fluorescent dyes were purchased from Molecular Probes (Eugene, OR, USA). Data were analyzed by laser confocal microscopy LSM510 Version 2.5 SP2 and presented as means ± SEM. The number of objective cells in each single experiment is 0–4. The number of cells or experiments is shown as n. Statistical analyses were performed using t-test or repeated ANOVA. A level of p<0.05 was
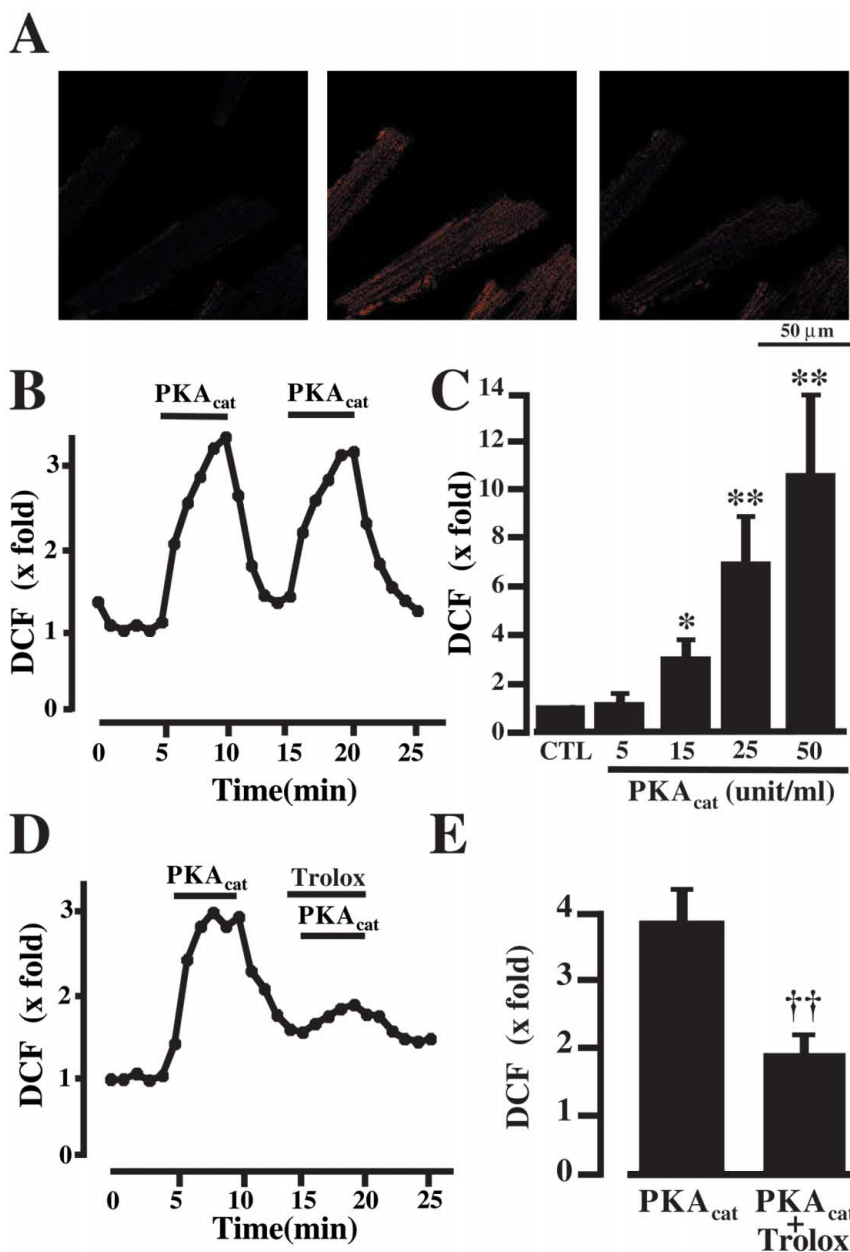
Fig 3. Effects of PKA$_{cat}$ on 2'7'-dichloro-fluorescin diacetate (DCF) fluorescence in permeabilized myocytes. (A) 2-D images of DCF were obtained before (Left), after administration (Center) and after the washout of 50 units/ml PKA$_{cat}$ (Right). (B) Representative recording of the changes in DCF fluorescence with 50 units/ml PKA$_{cat}$. (C) Dose-dependent effects of PKA$_{cat}$ on DCF fluorescence after 5 min perfusion of PKA$_{cat}$ (5–50 units/ml, n=8, 1–2 rats). (D) After the first administration and washout of PKA$_{cat}$ (50 units/ml), the second administration of PKA$_{cat}$ was repeated in the absence (B) and presence (D) of Trolox (100 μmol/L). (E) Changes in DCF fluorescence after 5 min of the first (PKA$_{cat}$) and second administrations of PKA$_{cat}$ with Trolox (PKA$_{cat}$ + Trolox) (n=6, 2 rats). Values are mean ± SEM. *p< 0.05 vs CTL by paired t-test. **p<0.01 vs CTL by paired t-test, ††p<0.01 vs PKA$_{cat}$ by paired t-test. See Figs 1,2 for other abbreviations.

accepted as statistically significant.

Results

Effects of PKA$_{cat}$ on FAD

To investigate whether PKA$_{cat}$ affects mitochondrial oxidative phosphorylation, the effects of PKA$_{cat}$ on FAD autofluorescence as an index of the mitochondrial redox state were examined in permeabilized myocytes. Fig 1A shows the time course of the changes in FAD fluorescence with 5, 25 and 50 units/ml of PKA$_{cat}$ and without PKA$_{cat}$. After 20 min perfusion of PKA$_{cat}$, 25 and 50 units/ml PKA$_{cat}$ reversibly increased FAD fluorescence by 13.0±5.6% (p< 0.01; n=8) and 56.6±7.9% (p<0.01; n=13), respectively. From these results, we used 50 units/ml of PKA$_{cat}$ in the following studies, unless stated differently.

When myocytes were pretreated with a PKA inhibitor fragment 14–24 trifluoroacetate salt (PKI; 20 and 80 μmol/L)

for 10 min and then PKA$_{cat}$ (50 units/ml) was added in the continuous presence of PKI, the PKA$_{cat}$-induced increase in FAD was significantly decreased to 31.8±3.5% (20 μmol/L; p<0.01 vs without PKI; n=10) and 15.7±5.8% (80 μmol/L; p<0.01 vs without PKI; n=5) after 20 min (Fig 1B). After 20 min administration of PKI alone, 20 and 80 μmol/L PKI did not alter FAD fluorescence (data not shown).

The BAR stimulation increases [Ca^{2+}]$_c$ and [Ca^{2+}]$_m$. The elevated [Ca^{2+}]$_m$ activates mitochondrial dehydrogenases, which alter the redox state of the mitochondrial matrix. Next, we investigated the effects of [Ca^{2+}]$_c$ on PKA$_{cat}$-induced changes in FAD fluorescence. FAD fluorescence was measured in both the presence (200 nmol/L) and absence of Ca^{2+} in the internal solution. As shown in Figs 1C and D, there were no significant changes of PKA$_{cat}$-induced FAD elevation in the presence or absence of Ca^{2+}, indicating the observed elevation of FAD fluorescence was not related to [Ca^{2+}]$_c$ (and probably [Ca^{2+}]$_m$).

Effects of PKA$_{cat}$ on $\Delta\psi_m$

In the next series of experiments, we examined the effects of PKA$_{cat}$ on $\Delta\psi_m$ by measuring the TMRE intensities. The 2-D images of TMRE before and after the administration of 50 units/ml PKA$_{cat}$ are shown in Figs 2A and B shows the concentration-dependent effects of PKA$_{cat}$ on the reduction of TMRE signal. PKA$_{cat}$-induced TMRE alterations were not observed at concentrations of PKA$_{cat}$ less than 15 units/ml. Fig 2C shows the time course of the change in TMRE intensities when PKA$_{cat}$ (50 units/ml) was administered, with or without PKI. The exposure to 50 units/ml PKA$_{cat}$ for 20 min reversibly decreased TMRE fluorescence to 48.1±9.5% of the control (p<0.01; n=6). When cells were pretreated with PKI, the PKA$_{cat}$-induced reduction of the TMRE signal was inhibited, and TMRE intensity decreased to 83.1±5.0% (20μmol/L; p<0.01 vs PKA$_{cat}$; n=6) and 88.9±9.5% (80μmol/L; p<0.01 vs PKA$_{cat}$; n=6) after 20 min.

To investigate the effect of Ca^{2+} in the PKA$_{cat}$-induced depolarization of $\Delta\psi_m$, the changes in PKA$_{cat}$-induced TMRE fluorescence were measured in the presence (200 nmol/L) and absence of Ca^{2+} in the internal solution. Fig 2D is a representative recording of TMRE fluorescence with and without Ca^{2+} in the internal solution. The data summarized in Fig 2E indicated that there was no difference in the PKA$_{cat}$-induced TMRE signal reduction with or without Ca^{2+} in the internal solution.

Effects of PKA on ROS Generation in Skinned Myocytes

It has been reported that βAR activation provokes oxidative stress in the heart,[17] so to assess whether PKA$_{cat}$ increases ROS generation in permeabilized myocytes, we examined the effect of PKA$_{cat}$ on DCF intensities.

The 2-D images of DCF before and after the administration of 50 units/ml PKA$_{cat}$ are shown in Figs 3A and B shows that exposure to 50 units/ml PKA$_{cat}$ reversibly increased DCF fluorescence. Dose-dependent effects of PKA$_{cat}$ on the increases in DCF intensity are summarized in Fig 3C. After 5 min perfusion, 15, 25 and 50 units/ml of PKA$_{cat}$ reversibly increased DCF fluorescence by 3.0±0.2 fold (p<0.05, n=8), 6.9±2.2 fold (p<0.01; n=8), and 10.5±3.3 fold (p<0.01; n=8), respectively.

As shown in Figs 3D and E, when cells were pretreated with a ROS scavenger (Trolox; 100μmol/L), the PKA$_{cat}$-induced DCF increase was significantly inhibited from 3.8±0.4 to 1.9±0.3 fold (p<0.01 vs PKA$_{cat}$; n=6). The PKA$_{cat}$-induced increase in the DCF signal was prevented by perfusion of 20μmol/L PKI (data not shown). These results indicated that perfusion of PKA$_{cat}$ in the permeabilized myocytes caused a concentration-dependent reversible generation of ROS in the mitochondrial matrix.

Effect of ROS Scavenger on PKA$_{cat}$-Induced FAD and $\Delta\psi_m$ Alteration

Next, to determine whether the generated ROS were involved in the regulation of the mitochondrial redox state and $\Delta\psi_m$ depolarization, the effects of Trolox on PKA$_{cat}$-induced FAD and $\Delta\psi_m$ alteration were examined. The time course of the changes in FAD fluorescence (Fig 4A) and TMRE fluorescence (Fig 4B) in the absence or presence of Trolox (10 and 100μmol/L) are shown; 100μmol/L Trolox decreased the PKA$_{cat}$-induced FAD elevation to 27.6±6.7% (p<0.01 vs PKA$_{cat}$; n=5) after 20 min. As for TMRE, 10 and 100μmol/L Trolox inhibited the PKA$_{cat}$-induced TMRE depression to 86.8±4.7% (100μmol/L; p<0.01 vs PKA$_{cat}$;
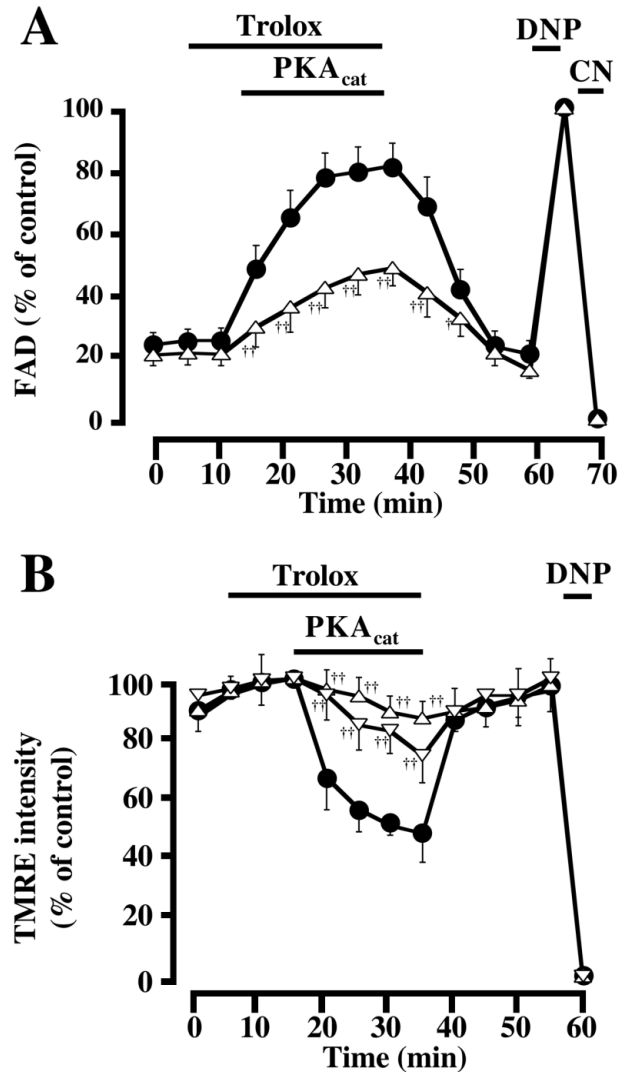
Fig 4. Effect of scavenger of reactive oxygen species (ROS) scavenger on PKA$_{cat}$-induced $\Delta\psi_m$ and FAD alteration. (A) Time course of the changes in FAD signal by 50 units/ml PKA$_{cat}$ with (●, n=5, 1 rat) or without (△, n=13, 4 rats) 100μmol/L Trolox. (B) Time course of the changes in TMRE intensity after the administration of PKA$_{cat}$ without (●, n=6, 2 rats) or with Trolox (▽, 100μol/L; n=8, 2 rats; ▽, 10μmol/L; n=7, 1 rat). Values are mean±SEM. †p<0.05 vs 50 units/ml PKA$_{cat}$ by ANOVA, ††p<0.01 vs 50 units/ml PKA$_{cat}$ by ANOVA. See Figs 1–3 for other abbreviations.

n=8) and 74.0±9.0% (10μmol/L; p<0.01 vs PKA$_{cat}$; n=7) of the control after 20 min, respectively.

Mechanism of PKA$_{cat}$-Induced $\Delta\psi_m$ Depolarization

Although the mechanism of the depolarization of $\Delta\psi_m$ in response to oxidative stress is not fully understood, previous studies have reported 2 possible candidates. Opening of either the mitochondrial permeability transition pore (mPTP)[18] or the mitochondrial inner membrane anion channel (IMAC)[19] is a possibility. To investigate the mechanism of PKA$_{cat}$-induced $\Delta\psi_m$ depolarization, we observed the effects of an mPTP inhibitor, cyclosporine A (CsA) and an IMAC inhibitor, 4,4'-diisothiocyanatostilbene-2,2'-disulfonic acid (DIDS) on PKA$_{cat}$-induced $\Delta\psi_m$ depolarization. We have previously reported that 100 nmol/L CsA inhibited the opening of the mPTP in our experimental conditions[20]

CsA or DIDS   **DNP**

PKA$_{cat}$

Fig 5.   Mechanism of PKA$_{cat}$-induced $\Delta\psi_m$ depolarization. Time course of the changes in the TMRE signal with PKA$_{cat}$ alone (●, 50 units/ml; n=13, 4 rats) with CsA (○, 100 nmol/L; n=10, 3 rats) or DIDS (◆, 1 μmol/L; n=7, 2 rats). Values are mean±SEM. †p<0.05 vs 50 units/ml PKA$_{cat}$ by ANOVA, ††p<0.01 vs 50 units/ml PKA$_{cat}$ by ANOVA. CSA, cyclosporine A; DIDS, 4,4'-diisothiocyanatostilbene-2,2'-disulfonic acid. See Figs 1–3 for other abbreviations.

Fig 5 demonstrates the time course of the changes in TMRE fluorescence in the presence of CsA (100 nmol/L) or DIDS (1 μmol/L). CsA did not alter the response of TMRE fluorescence to PKA$_{cat}$ (51.5±7.5%; n=10), whereas DIDS inhibited the PKA$_{cat}$-induced $\Delta\psi_m$ depolarization (89.1±4.0%; p<0.01; n=7) after 20 min. These results suggest that the ROS generated by PKA$_{cat}$ cause $\Delta\psi_m$ depolarization via DIDS-sensitive pathways.

Discussion

In the present study, we investigated the effects of PKA$_{cat}$ on the changes in FAD, $\Delta\psi_m$ and the generation of ROS in chemically skinned cardiac myocytes. Our results indicate that (1) PKA$_{cat}$ accelerated FAD oxidation and depolarized $\Delta\psi_m$, (2) PKA$_{cat}$ increased the production of ROS in the mitochondrial matrix, (3) scavenging ROS generation inhibited both the oxidation of FAD and the depolarization of $\Delta\psi_m$ induced by PKA$_{cat}$ and (4) PKA$_{cat}$-induced $\Delta\psi_m$ depolarization could be mediated by opening of the IMAC.

Measurements of Mitochondrial Function in Permeabilized Myocytes

Previous studies examining the effects of PKA$_{cat}$ on mitochondrial functions have been conducted mainly with isolated mitochondria[12,21,22] or direct injection of PKA$_{cat}$ into the cardiomyocyte[23] By using permeabilized myocytes, the condition of the extramitochondrial medium (ie, cytosolic Ca^{2+} and ATP concentrations) was controlled precisely, without changing the intracellular architecture[20,24,25] In intact myocytes, the stimulation of BAR increases [Ca^{2+}]$_i$ and the dynamic alteration in [Ca^{2+}]$_i$ leads to the changes in [Ca^{2+}]$_m$ and thus mitochondrial function. These effects of [Ca^{2+}]$_i$ were excluded in skinned myocytes. Interestingly, we observed that the effects of PKA$_{cat}$ on mitochondrial

function were independent of the Ca^{2+} concentration of the internal solution (Figs 1C,D, 2D,E). Although BAR stimulation is known to activate several intracellular signaling pathways, such as JNK, p38, and extracellar signal-regulated kinase[26] permeabilization of the cell membrane loses these cytosolic signaling messengers and proteins, and only the direct effects of PKA on mitochondrial function were examined in the present experimental conditions. It should be also considered that in permeabilized myocytes, the effects of PKA on glycolysis and fatty acid oxidation, which could affect mitochondrial metabolism, would be lost.

We demonstrated dose-dependent effects of PKA$_{cat}$ on FAD, $\Delta\psi_m$ and the generation of ROS. The concentrations of PKA$_{cat}$ used in this study were within the range reported in the literature[27,28] In the preliminary experiments, we found that the same concentrations of PKA$_{cat}$ in the pipette solution increased the voltage-dependent Ca^{2+} current of patch-clamped rat ventricular myocytes (data not shown).

PKA$_{cat}$-Induced ROS Generation in Mitochondria

It is known that BAR stimulation provokes oxidative stress, causing cardiac cell damage[17] which antioxidants prevent. There are several extra-mitochondrial sources of ROS and the assignment of the mitochondria as the site of ROS generation is not completely resolved[29–31] We demonstrated that PKA$_{cat}$ induced ROS generation and Trolox inhibited PKA$_{cat}$-induced ROS generation. Furthermore, PKA$_{cat}$-induced $\Delta\psi_m$ depolarization was also inhibited by another ROS scavenger, N-acetylcysteine (NAC; 400 μmol/L, data not shown). These results indicate that PKA$_{cat}$-induced $\Delta\psi_m$ depolarization is related to mitochondrial ROS production. Because DCF is not a specific dye for ROS and both NAC and Trolox are broad-spectrum ROS scavengers, it is difficult to identify which type of ROS was responsible for PKA$_{cat}$-induced $\Delta\psi_m$ depolarization.

For the mechanism of ROS generation by BAR stimulation, Singal et al reported that the oxidation of hydroxyl groups in catecholamines causes their conversion to quinines and that the subsequent formation of adenochromes accounts for the hazardous effects of catecholamines[9] Remondino et al reported that BAR activation rapidly provoked oxidative stress via the phosphorylation of JNK and p38 MAP kinases[8]

The ROS production in the mitochondria contributes to pathological process such as cardiomyopathy[32] aging[33] apoptosis[34] hypoxia[35] and ischemia/reperfusion[36,37] The complexes I and III of the mitochondrial electron transport chain (ETC) are regarded as the major sites of ROS production. It has been reported that PKA$_{cat}$ activates the respiratory chain complex I and/or III, and decreases the generation of ROS in isolated mitochondria[13,21,22] In contrast, our results showed that PKA$_{cat}$ caused an increase in ROS production in the mitochondrial matrix and that this effect of PKA$_{cat}$ on mitochondrial ROS production was independent of the cytosolic (and hence mitochondrial) Ca^{2+} concentration. The discrepancies between our results and those of previous studies might be related to difference in the materials used (skinned myocytes vs isolated mitochondria). Further investigation is needed to clarify the mechanism of PKA-induced ROS generation in cardiac myocytes.

PKA$_{cat}$-Induced $\Delta\psi_m$ Depolarization in Skinned Myocytes

We have shown that Trolox inhibited both the PKA$_{cat}$-induced FAD elevation and $\Delta\psi_m$ depolarization (Figs 4A,B),

suggesting that PKA$_{cat}$-induced ROS generation mediates mitochondrial metabolism.

Zorov et al demonstrated the phenomenon known as mitochondrial ROS-induced ROS release, in which rapid and spatio-temporally heterogeneous discharge of $\Delta\Psi_m$ in response to oxidative stress occurs with opening of the mPTP.[18] Bera et al reported that phosphorylation of the voltage-dependent anion channel by PKA$_{cat}$ reduced the magnitude and the opening probability of the single channel current, indicating that PKA could, at least in part, modulate mPTP.[38] Recently, Aon et al reported that a single local laser flash triggered synchronized and self-sustained oscillations in $\Delta\Psi_m$, NADH and ROS, which were related to the mitochondrial IMAC, but not to mPTP.[19] Our results that the inhibition of the IMAC by DIDS eliminated PKA$_{cat}$-induced $\Delta\Psi_m$ depolarization, whereas CsA did not (Fig 5), support the idea that depolarization of $\Delta\Psi_m$ by ROS could be related to opening of the IMAC. Furthermore, the PKA$_{cat}$-induced $\Delta\Psi_m$ depolarization was also inhibited by inhibitors of the mitochondrial benzodiazepine receptor, 4'-chloro-diazepam (50μmol/L) and PK11195 (50μmol/L), which have been reported to suppress the IMAC more selectively than DIDS[19] (data not shown).

AKAPs are located in the outer mitochondrial membrane and the molecular weight of PKA$_{cat}$ (38kDa) is too large for it to cross the outer membrane. Therefore, it seems necessary to transform the signal from phosphorylated proteins to the ETC, but the precise signaling cascade from the outer mitochondrial membrane to the ETC remains to be elucidated.

As for the mechanism of PKA-induced $\Delta\Psi_m$ depolarization, the contribution of FoF$_1$-ATPase, Ca^{2+}-activated K$^+$ channels and uncoupling proteins should be also considered. Oligomycin, a FoF$_1$-ATPase inhibitor, did not affect PKA-induced $\Delta\Psi_m$ depolarization or ROS generation in our experiments (data not shown), which indicates that the activity of FoF$_1$-ATPase was unchanged in our experiments.

Recently, it was reported that PKA modulates the opening of the mitochondrial Ca^{2+}-activated K$^+$ channel, depolarizes $\Delta\Psi_m$ and attenuates the mitochondrial Ca^{2+} overload.[39] Because PKA$_{cat}$-induced alterations in FAD, $\Delta\Psi_m$ and ROS generation were independent of Ca^{2+} concentration in the present study, there might be less connection between our results and Ca^{2+}-activated K$^+$ channels. The functional relationship between the Ca^{2+}-activated K$^+$ channel and the IMAC remains to be investigated.

Finally, it has been shown that ROS can stimulate mitochondrial uncoupling protein, which could depolarize $\Delta\Psi_m$. However, the activation of uncoupling protein is inhibited by 100μmol/L of ATP.[40] Our internal solution contained 2mmol/L ATP, which would profoundly suppress the activity of the uncoupling protein. It is, therefore, unlikely that PKA-induced $\Delta\Psi_m$ depolarization was related to mitochondrial uncoupling protein in our experiments.

Clinical Implication

It is known that a short exposure to massive concentrations of catecholamines causes reversible left ventricular dysfunction,[41] and that chronic exposure to β-adrenergic stimulation leads to progression of irreversible myocardial dysfunction in heart failure.

The mechanisms of the toxic effects of norepinephrine include (1) relative hypoxia because of increased cardiac work, (2) cytosolic and mitochondrial Ca^{2+} overload and (3) formation of oxidative catecholamine metabolites.[42,43] The myocardial cell damage caused by excessive β-adrenergic stimulation is inhibited by antioxidative interventions.[9] Our findings that a high concentration of PKA caused both $\Delta\Psi_m$ depolarization and ROS production suggest another explanation of the impaired cardiac function after exposure to excessive levels of catecholamines. On the other hand, a lower concentration of PKA induced a small increase in ROS generation and little change in $\Delta\Psi_m$ depolarization. It has been reported that ROS could act as a second messenger in response to the stimulation of intracellular signaling pathways and protect myocytes from pathological conditions such as ischemia/reprefusion injury.[44,45] Thus, it is also necessary to consider that ROS (induced by the stimulation of BAR) in adequate amounts have beneficial effects on myocardial function.

Conclusion

We demonstrated that in permeabilized myocytes PKA regulated the mitochondrial redox state and $\Delta\Psi_m$ via mitochodrial ROS generation, and that the PKA-induced $\Delta\Psi_m$ depolarization was not related to mPTP, but to DIDS-sensitive mechanisms, which could be the IMAC. The depolarization of $\Delta\Psi_m$ by PKA suggests a direct effect of PKA on mitochondrial function and could explain mitochondrial dysfunction under the condition of extensive BAR stimulation, such as in chronic heart failure.

References

1. McDonald TF, Pelzer S, Trautwein W, Pelzer DJ. Regulation and modulation of calcium channels in cardiac, skeletal, and smooth muscle cells. *Physiol Rev* 1994; **74:** 365–507.
2. Lindemann JP, Jones LR, Hathaway DR, Henry BG, Watanabe AM. β-Adrenergic stimulation of phospholamban phosphorylation and Ca^{2+}-ATPase activity in guinea pig ventricles. *J Biol Chem* 1983; **258:** 464–471.
3. Takasago T, Imagawa T, Shigekawa M. Phosphorylation of the cardiac ryanodine receptor by cAMP-dependent protein kinase. *J Biochem (Tokyo)* 1989; **106:** 872–877.
4. Hasking GJ, Esler MD, Jennings GL, Burton D, Johns JA, Korner PI. Norepinephrine spillover to plasma in patients with congestive heart failure: Evidence of increased overall and cardiorenal sympathetic nervous activity. *Circulation* 1986; **73:** 615–621.
5. Reiken S, Gaburjakova M, Gaburjakova J, He KL, Prieto A, Becker E, et al. β-adrenergic receptor blockers restore cardiac calcium release channel (ryanodine receptor) structure and function in heart failure. *Circulation* 2001; **104:** 2843–2848.
6. Somani P, Laddu AR, Hardm HF. Nutritional circulation in the heart. 3: Effect of isoproterenol and, adrenergic blockade on myocardial hemodynamics and rubicium-86 extraction in the isolated supported heart preparation. *J Pharmacol Exp Ther* 1970; **175:** 577–592.
7. Uyemura SA, Curti C. Respiration and mitochondrial ATPase in energized mitochondria during isoproterenol-induced cell injury of myocardium. *Int J Biochem* 1991; **23:** 1143–1149.
8. Remondino A, Kwon SH, Communal C, Pimentel DR, Sawyer DB, Singh K, et al. β-adrenergic receptor-stimulated apoptosis in cardiac myocytes is mediated by reactive oxygen species/c-Jun NH2-terminal kinase-dependent activation of the mitochondrial pathway. *Circ Res* 2003; **92:** 136–138.
9. Singal PK, Kapur N, Dhillon KS, Beamish RE, Dhalla NS. Role of free radicals in catecholamine-induced cardiomyopathy. *Can J Physiol Pharmacol* 1982; **60:** 1390–1397.
10. Kametani R, Miura T, Harada N, Shibuya M, Wang R, Tan H, et al. Carvedilol inhibits mitochondrial oxygen consumption and superox-

ide production during calcium overload in isolated heart mitochondria. *Circ J* 2006; **70:** 321–326.

11. Wang L, Sunahara RK, Krumins A, Perkins G, Crochiere ML, Mackey M, et al. Cloning and mitochondrial localization of full-length D-AKAP2, a protein kinase A anchoring protein. *Proc Natl Acad Sci USA* 2001; **98:** 3220–3225.

12. Papa S. The NDUFS4 nuclear gene of complex I of mitochondria and the cAMP cascade. *Biochim Biophys Acta* 2002; **1555:** 147–153.

13. Technikova-Dobrova Z, Sardanelli AM, Speranza F, Scacco S, Signorile A, Lorusso V, et al. Cyclic adenosine monophosphate-dependent phosphorylation of mammalian mitochondrial proteins: Enzyme and substrate characterization and functional role. *Biochemistry* 2001; **40:** 13941–13947.

14. Nomura N, Satoh H, Terada H, Matsunaga M, Watanabe H, Hayashi H. CaMKII-dependent reactivation of SR Ca^{2+} uptake and contractile recovery during intracellular acidosis. *Am J Physiol Heart Circ Physiol* 2002; **283:** H193–H203.

15. Hayashi H, Miyata H, Noda N, Kobayashi A, Hirano M, Kawai T, et al. Intracellular Ca^{2+} concentration and pHi during metabolic inhibition. *Am J Physiol* 1992; **262:** C628–C634.

16. Katoh H, Nishigaki N, Hayashi H. Diazoxide opens the mitochondrial permeability transition pore and alters Ca^{2+} transients in rat ventricular myocytes. *Circulation* 2002; **105:** 2666–2671.

17. Zhang GX, Kimura S, Nishiyama A, Shokoji T, Rahman M, Yao L, et al. Cardiac oxidative stress in acute and chronic isoproterenol-infused rats. *Cardiovasc Res* 2005; **65:** 230–238.

18. Zorov DB, Filburn CR, Klotz LO, Zweier JL, Sollott SJ. Reactive oxygen species (ROS)-induced ROS release: A new phenomenon accompanying induction of the mitochondrial permeability transition in cardiac myocytes. *J Exp Med* 2000; **192:** 1001–1014.

19. Aon MA, Cortassa S, Marban E, O'Rourke B. Synchronized whole cell oscillations in mitochondrial metabolism triggered by a local release of reactive oxygen species in cardiac myocytes. *J Biol Chem* 2003; **278:** 44735–44744.

20. Saotome M, Katoh H, Satoh H, Nagasaka S, Yoshihara S, Terada H, et al. Mitochondrial membrane potential modulates regulation of mitochondrial Ca^{2+} in rat ventricular myocytes. *Am J Physiol Heart Circ Physiol* 2005; **288:** H1820–H1828.

21. Maj MC, Raha S, Myint T, Robinson BH. Regulation of NADH/CoQ oxidoreductase: Do phosphorylation events affect activity? *Protein J* 2004; **23:** 25–32.

22. Raha S, Myint AT, Johnstone L, Robinson BH. Control of oxygen free radical formation from mitochondrial complex I: Roles for protein kinase A and pyruvate dehydrogenase kinase. *Free Radic Biol Med* 2002; **32:** 421–430.

23. Osterrieder W, Brum G, Hescheler J, Trautwein W, Flockerzi V, Hofmann F. Injection of subunits of cyclic AMP-dependent protein kinase into cardiac myocytes modulates Ca^{2+} current. *Nature* 1982; **298:** 576–578.

24. Lukyanenko V, Gyorke S. Ca^{2+} sparks and Ca^{2+} waves in saponin-permeabilized rat ventricular myocytes. *J Physiol* 1999; **521:** 575–585.

25. Matsunaga M, Saotome M, Satoh H, Katoh H, Terada H, Hayashi H. Different actions of cardioprotective agents on mitochondrial Ca^{2+} regulation in a Ca^{2+} paradox-induced Ca^{2+} overload. *Circ J* 2005; **69:** 1132–1140.

26. Takemoto Y, Yoshiyama M, Takeuchi K, Omura T, Komatsu R, Izumi Y, et al. Increased JNK, AP-1 and NF-κB DNA binding activities in isoproterenol-induced cardiac remodeling. *J Mol Cell Cardiol*

1999; **31:** 2017–2030.

27. Saeki Y, Kobayashi T, Minamisawa S, Sugi H. Protein kinase A increases the tension cost and unloaded shortening velocity in skinned rat cardiac muscle. *J Mol Cell Cardiol* 1997; **29:** 1655–1663.

28. Terentyev D, Viatchenko-Karpinski S, Gyorke I, Terentyeva R, Gyorke S. Protein phosphatases decrease sarcoplasmic reticulum calcium content by stimulating calcium release in cardiac myocytes. *J Physiol* 2003; **552:** 109–118.

29. Kooij A. A re-evaluation of the tissue distribution and physiology of xanthine oxidoreductase. *Histochem J* 1994; **26:** 889–915.

30. Mueller S, Weber A, Fritz R, Mutze S, Rost D, Walczak H, et al. Sensitive and real-time determination of H_2O_2 release from intact peroxisomes. *Biochem J* 2002; **363:** 483–491.

31. Souza HP, Liu X, Samouilov A, Kuppusamy P, Laurindo FR, Zweier JL. Quantitation of superoxide generation and substrate utilization by vascular NAD(P)H oxidase. *Am J Physiol Heart Circ Physiol* 2002; **282:** H466–H474.

32. Ishikawa K, Kimura S, Kobayashi A, Sato T, Matsumoto H, Ujiie Y, et al. Increased reactive oxygen species and anti-oxidative response in mitochondrial cardiomyopathy. *Circ J* 2005; **69:** 617–620.

33. Herrero A, Barja G. Sites and mechanisms responsible for the low rate of free radical production of heart mitochondria in the long-lived pigeon. *Mech Ageing Dev* 1997; **98:** 95–111.

34. Kumar D, Lou H, Singal PK. Oxidative stress and apoptosis in heart dysfunction. *Herz* 2002; **27:** 662–668.

35. Becker LB, vanden Hoek TL, Shao ZH, Li CQ, Schumacker PT. Generation of superoxide in cardiomyocytes during ischemia before reperfusion. *Am J Physiol* 1999; **277:** H2240–H2246.

36. Lesnefsky EJ, Moghaddas S, Tandler B, Kerner J, Hoppel CL. Mitochondrial dysfunction in cardiac disease: Ischemia/reperfusion, aging, and heart failure. *J Mol Cell Cardiol* 2001; **33:** 1065–1089.

37. Almsherqi ZA, McLachlan CS, Kostetski I, Lai CS, Chiu CC, Liu SL, et al. Displacement of the beating heart induces an immediate and sustained increase in myocardial reactive oxygen species. *Circ J* 2006; **70:** 1226–1228.

38. Bera AK, Ghosh S. Dual mode of gating of voltage-dependent anion channel as revealed by phosphorylation. *J Struct Biol* 2001; **135:** 67–72.

39. Sato T, Saito T, Saegusa N, Nakaya H. Mitochondrial Ca^{2+}-activated K^+ channels in cardiac myocytes: A mechanism of the cardioprotective effect and modulation by protein kinase A. *Circulation* 2005; **111:** 198–203.

40. Echtay KS, Roussel D, St-Pierre J, Jekabsons MB, Cadenas S, Stuart JA, et al. Superoxide activates mitochondrial uncoupling proteins. *Nature* 2002; **415:** 96–99.

41. Akashi YJ, Nakazawa K, Sakakibara M, Miyake F, Koike H, Sasaka K. The clinical features of takotsubo cardiomyopathy. *Q J Med* 2003; **96:** 563–573.

42. Mann DL, Kent RL, Parsons B, Cooper Gt. Adrenergic effects on the biology of the adult mammalian cardiocyte. *Circulation* 1992; **85:** 790–804.

43. Crompton M. The mitochondrial permeability transition pore and its role in cell death. *Biochem J* 1999; **341:** 233–249.

44. Ambrosio G, Tritto I, Chiariello M. The role of oxygen free radicals in preconditioning. *J Mol Cell Cardiol* 1995; **27:** 1035–1039.

45. Yaguchi Y, Satoh H, Wakahara N, Katoh H, Uehara A, Terada H, et al. Protective effects of hydrogen peroxide against ischemia/reperfusion injury in perfused rat hearts. *Circ J* 2003; **67:** 253–258.